

Radioimmunolocalization of Metastatic Breast Carcinoma Using Indium-111-Methyl Benzyl DTPA BrE-3 Monoclonal Antibody: Phase I Study

Elissa Lipcon Kramer, Sally J. DeNardo, Leonard Liebes, Linda A. Kroger, Marilyn E. Noz, Howard Mizrahi, Qansy A. Salako, Philip Furmanski, Stephan D. Glenn, Gerald L. DeNardo and Roberto Ceriani

Division of Nuclear Medicine, Kaplan Comprehensive Cancer Center, Division of Oncology, Department of Pathology, NYU Medical Center/Bellevue Hospital Center, New York, New York; Department of Biology, New York University, New York, New York; Section of Radiodiagnosis and Therapy, University of California at Davis, Sacramento, California; Coulter Immunology, Hialeah, Florida; and Cancer Research Fund of Contra Costa, Walnut Creek, California

Pharmacokinetics of radiolabeled BrE-3 monoclonal antibody (Mab), reactive against a breast mucin epitope, were assessed in 15 patients with advanced breast cancer. Patients received 5 mCi (185 MBq) of ^{111}In -methyl benzyl isothiocyanate DTPA (MX-DTPA) conjugated BrE-3 Mab intravenously with total antibody doses of 10, 50 or 100 mg. Serial quantitative imaging, blood and urine clearance were obtained to measure pharmacokinetics, assess tumor localization and estimate radiation dose. Organ function was followed to determine toxicity. Mild allergic reactions occurred in four patients. Eighty-six percent of 70 known lesions and 5 unsuspected lesions were detected by antibody imaging. Biexponential modeling of radiolabeled antibody in serum showed a $T_{1/2\alpha} = 9.5 \pm 2.7$ hr and $T_{1/2\beta} = 56 \pm 25.4$ hr. Total urinary excretion averaged $35.5\% \pm 19.3\%$ injected dose (ID) by Day 8. Quantitative imaging showed that 0.02–2.56 %ID localized in tumors. Extrapolating dosimetry from ^{111}In -MX-DTPA-BrE-3 to ^{90}Y -MX-DTPA-BrE-3, we estimate therapeutic radiation doses could be delivered to some tumors with tolerable toxicity.

J Nucl Med 1993; 34:1067–1074

Radioimmunolocalization studies in breast cancer have employed tumor-directed antibodies reactive to a number of breast carcinoma associated antigens. Two of the most frequently targeted have included carcinoembryonic antigen (1–5) and human milk fat globule membrane-associated antigen (HMFG) (6–10), the breast epithelial mucin (11). Because HMFG-associated antigen is often abundantly expressed on human breast cancers, antibodies directed against epitopes of this substance offer a logical vehicle for

delivery of radioisotopes to these cancers for either imaging or therapy.

Recently, a series of antibodies (11–12) has been developed which recognizes the 400 kD mucin present in HMFG (12). This mucin was detected by these antibodies in >90% of breast cancer cell lines (13) and in most breast carcinoma specimens examined (12). The molecule of breast epithelial mucin has a central moiety comprising up to 60 tandem repeat sequences of 20 amino acids with unique amino and carboxy terminal regions. It is this polyepitopic tandem repeat against which most, if not all, monoclonal antibodies (Mabs) specific for breast mucin are reactive.

Biodistribution studies with two of these Mabs, Mc-5 and BrE-3, demonstrated their ability to accumulate in human breast cancer grown in nude mice (14). Subsequent preclinical studies have shown them to be successful agents in mouse xenograft radioimmunotherapy (15,16). Initial clinical trials with Mc-5 showed significant complexing of the antibody with a circulating epitope (17). Little tumor localization was seen despite the in vitro demonstration of antigen on breast carcinoma. Mab BrE-3, which also has been effective in experimental mouse xenograft radioimmunotherapy, recognizes an epitope less frequently and less abundantly present in the serum (18). For this reason, a Phase I clinical study using ^{111}In -MX-DTPA-BrE-3 was undertaken to determine the pharmacokinetics, tumor localization and toxicity of this radioimmunoconjugate.

MATERIALS AND METHODS

Subjects

In this protocol, 15 women, average age 59 yr (range 42–80 yr), with metastatic or recurrent breast cancer were studied. All patients had been treated previously for their metastatic or recurrent disease with chemotherapy (n = 13), radiation (n = 7) and/or hormonal therapy (n = 10). In each patient, the expression of the antigen recognized by BrE-3 was established on previously ex-

Received Nov. 4, 1992; revision accepted Mar. 19, 1993.

For correspondence and reprints contact: Elissa Kramer, MD, Division of Nuclear Medicine HW215, NYU Medical Center, 560 First Ave., New York, NY 10016.

TABLE 1
Known Disease: Detection Rates

(No. positive on scan/No. of known lesions)		
Site	No. of lesions	No. of patients
Bone	39/43* (91%)	7/7 (100%)
Liver	1/5 (20%)	1/4 (25%)
Lymph nodes	7/8 (88%)	6/6 (100%)
Lung	3/4 (75%)	3/4 (75%)
Chest wall	6/6 (100%)	6/6 (100%)
Pleura	2/2 (100%)	2/2 (100%)
Other (adrenal)	2/2 (100%)	2/2 (100%)
Overall	60/70 (86%)	12/15 (80%)

*Five previously unsuspected metastatic foci were detected by antibody imaging and subsequently confirmed by conventional imaging modalities; an additional six skeletal foci on antibody imaging could not be confirmed radiographically.

cised or biopsied tumor tissue using immunohistochemistry. Informed consent was obtained according to the guidelines established by the institutional review boards at the respective institutions. Normal renal, hepatic, hematologic and cardiac function were established by blood tests and electrocardiograms. Routine radiographic and scintigraphic studies, including plain film, CT, MRI and bone scan, were also obtained to establish the extent of disease. Sites of known disease included bone, liver, lung, chest wall, lymph nodes and adrenals (Table 1). Baseline human anti-mouse antibody (HAMA) and serum levels of antigen recognized by BrE-3 were measured.

Immunohistochemistry

Immunohistochemical analysis for BrE-3 epitope was performed on tissue samples from breast and lymph node specimens using a modified avidin-biotin-peroxidase technique (Vectastain ABC, Burlingame, CA). BrE-3 antibody (Coulter Immunology, Hialeah, FL) was supplied in a concentration of 46.73 mg/ml. Dilutions from 1:100 to 1:25 were applied to formalin-fixed paraffin embedded sections on poly-L-lysine coated slides. Stained sections were evaluated for percent cells stained and intensity of staining (1 to 4+).

BrE-3 Antibody

BrE-3 antibody is a murine IgG₁ Mab which reacts with a polyepitopic 400 kD moiety of breast epithelial mucin (12). The antibody was developed at the Cancer Research Fund of Contra Costa (CRF) and has been shown to react with over 90% of breast carcinomas tested by immunopathology (12) as well as pancreatic and ovarian carcinoma. It shows minimal cross-reactivity with normal breast tissue (12).

The antibody was provided in human use form by Coulter Immunology (Division of Coulter Corporation, Hialeah, FL) as a sterile, low-pyrogen solution in both its unconjugated form and as BrE-3 antibody conjugated with (1,4) methyl-benzyl isothiocyanate DTPA (MX-DTPA) for labeling with ¹¹¹In-chloride.

Radiolabeling

Approximately 5 mCi (185 MBq) of pharmaceutical grade ¹¹¹In-chloride (Amersham Corp) was buffered in acetate, incubated with 2 mg MX-DTPA-BrE-3 for 20 min at room temperature and challenged with 5 mM EDTA. Instant thin-layer chromatography was performed to determine percent radioactivity present as ¹¹¹In-

MX-DTPA-BrE-3. This averaged 97% ± 6%. The antibody preparation was then mixed with 8 mg of unconjugated BrE-3, filtered through a 0.22 μ filter and diluted to 200 ml in 5% HSA in normal saline. Pyrogen and sterility testing was performed for each labeled preparation. Pyrogen levels in the antibody preparations were always within acceptable limits (<5 endotoxin units/kg/hr of infusion). All preparations were shown to be sterile. Immunoreactivity was assessed using BrE-3 antigen-coated beads and averaged 71% (range 56.5%–88%).

Antibody Administration

Total antibody doses of 10 mg, 50 mg or 100 mg were administered to cohorts of 5 patients each. For the patients at the 10-mg dose level, the radiolabeled antibody mixture was administered over 1 hr. In those patients who received the higher dose levels, the appropriate amount of unlabeled antibody in 5% HSA was administered intravenously at a rate of 1–2 mg/min followed by a wait of 30 min, and then by the radiolabeled antibody infusion over 1 hr.

To evaluate toxicity, vital signs were monitored for 3 hr from the beginning of the infusion. In addition, repeat blood chemistries, blood count, PT and PTT were obtained 72 hr after antibody administration.

Pharmacokinetics

Serial blood samples were performed at 5, 30, 60 min, and 2, 4 and 6 hr after the end of infusion and then daily for the next week. Timed urine collections were performed also through the eighth day following antibody administration for measurement of radioactivity. Serum and urine samples were counted to determine total radioactivity. Serum samples were further subjected to molecular size analysis, high-performance liquid chromatography (HPLC) to identify antigen antibody complexes, intact antibody and breakdown products. Samples (50–200 μl) were applied to a 10 mm × 50 cm BioRad TSK column equilibrated with 0.050 M NaH₂PO₄, 0.1 M Na₂SO₄ buffer (pH 6.8) with an elution flow rate of 0.6–1 ml/min. Detection was at 280 nm and 0.6–1 ml fractions were collected. Determination of radioactivity was performed either by flowing through a radiation detector or by counting of fractions in an LKB model 1282 gamma counter. The column calibration was verified using a 20-μl injection of Bio-Rad gel filtration standard (thyroglobulin, bovine gamma globulin, chicken ovalbumin, equine myoglobin, vitamin B-12).

Blood clearance of radiolabeled antibody as well as total urinary excretion of radioactivity were determined. The half-time for clearance of the radiolabeled antibody was determined using a nonlinear biexponential pharmacokinetic model. Initial parameter estimates were obtained using the Jana curve stripping algorithm (Statistical Consultants, Lexington, KY). These estimates were then applied to a biexponential model in PCNONLIN (Statistical Consultants, Lexington, KY) to fit the time/concentration antibody data with respect to the duration of the infusion as well as the intravenous route of administration. The key pharmacokinetic parameters obtained included half-lives for each compartment (e.g., alpha and beta) and the area under the concentration versus time curve (AUC).

Pharmacokinetic parameters, including T_{1/2α}, T_{1/2β} and AUC were compared among dose levels using an analysis of variance. Correlations of these parameters with dose level and antigen levels were examined.

Imaging

Quantitative planar imaging was performed to determine pharmacokinetics and tumor localization (19,20). All images were obtained using a large field of view gamma camera fitted with a medium-energy collimator. Prior to administration of the radiolabeled antibody, an ^{111}In transmission scan of the entire body was acquired. After administration of the antibody, anterior and posterior whole-body images as well as regional views of the head, chest, abdomen and pelvis were obtained at 4 hr after injection and on a minimum of three subsequent days up to 1 wk after infusion. Dual-energy windows centered on the 173 and 247 keV energy peaks of ^{111}In were employed. Regional spot views were acquired for 5 min per image or for 1×10^6 counts at the first three imaging sessions and for 7.5–10 min per view in the last imaging session. Typically, $1\text{--}3.5 \times 10^6$ counts were obtained in the early trunk views and $0.5\text{--}1.5 \times 10^6$ counts at the later time points.

Images were interpreted by the nuclear medicine physicians at each institution with full knowledge of the known extent of disease. Only those lesions which showed increased uptake, even in the liver, were considered positive. Cold liver lesions were not interpreted as positive for tumor. Because this was an early Phase I study whose purpose was to assess radioimmunoconjugate localization in known tumors, blinded readings of scans were not performed.

Regions of interest and background templates were generated over normal organs and tumors and applied to all imaging time points. Background subtraction and attenuation correction were performed for each region (19,20). For large organs, i.e., liver, spleen and lung, the geometric mean was determined. For kidney and for tumors, the counts from a single planar view were treated as a point source (20). Percent injected dose was determined and the effective half-life of the radiolabeled antibody for each organ, the whole body and tumors was calculated. The cumulative activity ($\mu\text{Ci}\cdot\text{hr}$) was calculated using the camera sensitivity derived from an ^{111}In standard of known activity.

The MIRDOSE2 formalism was applied using an implementation of the MIRDOSE2 program (Oak Ridge, TN) (22) to estimate radiation dosimetry for the $^{111}\text{In}\text{-MX-DTPA-BrE-3}$ and with extrapolation from the ^{111}In biodistribution data dosimetry for $^{90}\text{Y}\text{-MX-DTPA-BrE-3}$.

Blood dose to marrow was calculated using the concentration of activity in blood, assuming that 25% of the marrow volume was blood and using the "S" factor for marrow dose from marrow (nonpenetrating). For ^{111}In , this calculated dose was added to the dose to marrow from other organs and from the whole body to obtain an estimate of marrow dose (21). For ^{90}Y , the radiation dose from other organs or the whole body was not included since ^{90}Y penetrating radiation from these sites to the marrow contributes <1% of the total marrow dose.

Radiation tumor dose from radioactivity accumulation in tumor was calculated for measurable lesions using the appropriate "S" factors for ^{90}Y (23,24).

Measurement of Serum Levels of Breast Epithelial Mucin Binding to BrE-3

Serum samples for measurement of circulating breast mucin epitope reactive with BrE-3 were obtained prior to antibody administration. Serum samples were frozen at -20°C and sent to CRF for analysis. Circulating BrE-3 epitope was determined by a competitive serum assay with the BrE-3 epitope on the solid phase. Microtiter plates precoated with a source of BrE-3 epitope were presented with stoichiometric quantities of BrE-3 and serum

added in adequate dilution. After an overnight incubation, BrE-3 bound to the solid phase was detected by a radioiodinated anti-mouse immunoglobulin. Results obtained were compared to a standard curve and expressed as $\mu\text{g}/\text{ml}$ of protein equivalent breast epithelial mucin.

HAMA

HAMA was measured at baseline, 1 wk, 1 mo and 2–6 mo after administration of BrE-3 antibody. Both human IgG and IgE anti-mouse levels were measured in serum samples at Coulter Immunology. For determination of human IgG anti-mouse, serum samples were mixed with fixed Staph A bacteria and incubated to capture the IgG fraction of the human serum. The immunoglobulin-coated Staph A particles were then saturated with normal human immunoglobulin and incubated with ^{125}I -labeled BrE-3. The Staph A particles were then washed, pelleted by centrifugation and counted in a well-type gamma counter. The quantity of IgG anti-mouse was estimated using affinity-purified immunoglobulin from immunized cynomolgous monkeys as the standard.

Human IgE and IgE anti-mouse were estimated using 6.4-mm polystyrene beads coated with specific goat anti-human IgE to capture the IgE fraction of patient serum samples. For determination of human IgE levels, the beads were washed, incubated overnight with ^{125}I -labeled specific goat anti-human IgE immunoglobulin, washed and counted in a gamma counter. For measurement of human IgE-anti-mouse, the beads were washed, incubated overnight with ^{125}I -labeled BrE-3, washed and counted. The presence of human IgE anti-mouse was confirmed by repeating the assay using samples that had been treated by incubation at 56°C for 2 hr. To confirm the presence of human IgE anti-mouse, the concentration of anti-BrE-3 must drop at least 15% after heat treatment (25).

RESULTS

Toxicity

Very mild allergic reactions were observed in 3/15 patients: two Grade 1 (rash), one Grade 2 (mild laryngospasm). In one of these patients, the reaction seemed to be related to a rapid rate of infusion and abated with slowing of the infusion. One of these patients developed a single hive which resolved spontaneously. In a fourth patient, a 1-g drop in hemoglobin was observed, possibly due to blood drawing. In another patient, a transient mild elevation (Grade 1) in liver function tests was observed.

Immunohistochemistry

Immunohistochemical staining for BrE-3 epitope on tumor tissue was positive for all patients prior to entry into the study. In all patients entered, at least one tumor sample showed greater than 60% of the cells positive for the BrE-3 antigen.

Pharmacokinetics

The biodistribution data and biological half-time for radiolabeled antibody in normal organs is detailed in Table 2. At 72 hr, an average of $11.9\% \pm 5.2\%$ ID accumulated in the liver. By one week, an average of $5.8 \pm 2.7\%$ ID remained in the liver. Lung uptake at 72 hr averaged $5.0\% \pm 3.4\%$ ID and decreased by 1 wk. There was no significant difference in the %ID in the liver or lung among the different antibody dose levels ($p > 0.10$).

TABLE 2
Biodistribution/Organ Pharmacokinetics

	4 hr(%ID) (mean ± s.d.)	24 hr(%ID) (mean ± s.d.)	72 hr(%ID) (mean ± s.d.)	8 days(%ID) (mean ± s.d.)	T _{1/2β} (hr) (mean ± s.d.)
Liver	10.2 ± 3.6	12.5 ± 5.1	11.9 ± 5.2	5.8 ± 2.7	209.6 ± 153.1
Spleen	1.6 ± 0.7	1.7 ± 0.8	1.44 ± 0.7	0.8 ± 0.6	150.2 ± 80.1
Kidney	1.3 ± 0.6	1.5 ± 0.8	1.4 ± 0.6	0.7 ± 0.3	150.8 ± 98.7
Lungs	6.3 ± 2.0	6.0 ± 2.4	5.0 ± 3.4	1.9 ± 2.3	140.0 ± 120.6

In visualized tumors, an average uptake of 0.48% ± 0.59% ID (range 0.02%–2.56% ID) was measured by region of interest analysis of images. The T_{1/2β} for tumors averaged 194.4 ± 155 hr (range 45–804 hr).

Radiation dosimetry estimates were made for ¹¹¹In-BrE-3 from the imaging data (Table 3). Based on these estimates, the liver and spleen received the highest mean dose, 1.30 ± 0.46 rads/mCi and 1.48 ± 0.85 rads/mCi, respectively. Whole-body and marrow doses averaged 0.45 ± 0.11 and 0.48 ± 0.29 rads/mCi administered.

HPLC analysis of serum samples from 10 patients showed that >90% of the radioactivity in serum was associated with molecules of 150 kD. In the five remaining patients, at least 20% of the radioactivity was seen at ≥450 kD (Table 4), presumably representing high molecular weight antigen-antibody complexes. In these five patients, high molecular weight complexes were apparent immediately following the end of infusion. In four of these five patients, peak levels of complex occurred at the end of infusion. Very low levels of high molecular weight complexes were seen in seven additional patients. These appeared at various times after infusion and were usually transient.

A biexponential model was applied to the half-time for radiolabeled antibody in serum (Table 5). Mean half-life of the distribution phase (T_{1/2α}) was found to be 9.5 hr ± 2.7 hr. The mean half-life of the elimination phase (T_{1/2β}) was 56 ± 25.4 hr. The mean clearance of radiolabeled antibody from serum was 0.52 ± 0.09 ml/min/m². The mean percent of the AUC cleared with the half-life of the beta phase was 83.7% ± 2.3%. These parameters did not differ significantly among dose levels of antibody (p > 0.2). However,

TABLE 3
Radiation Dosimetry Estimates (rad/mCi)

Organ	¹¹¹ In dose (mean ± s.d.)	⁹⁰ Y dose equivalent (mean ± s.d.)
Kidneys	0.83 ± 0.74	6.47 ± 6.46
Liver	1.30 ± 0.46	9.21 ± 3.67
Lungs	0.95 ± 0.46	8.42 ± 5.93
Spleen	1.48 ± 0.85	15.36 ± 10.96
Whole body	0.45 ± 0.11	2.03 ± 1.60
Total marrow	0.48 ± 0.29	2.10 ± 0.97
Blood to marrow	0.19 ± 0.09	2.10 ± 0.97
WB to marrow	0.29 ± 0.22	*

*Whole body (WB) contributes <1% of the ⁹⁰Y dose to marrow.

there was significant correlation between the AUC (μg/ml/hr) and the dose of antibody administered (R² = 0.99).

Total urinary excretion through 8 days postinfusion averaged 35.5% ± 19.3 %ID for the 15 patients.

Imaging Results

Seventy sites of known disease were identified by conventional diagnostic techniques prior to the antibody imaging study: 43 in bone, 5 liver, 6 chest wall, 8 lymph nodes and 8 in other organs. Eighty-six percent of these previously known lesions were identified on the scans (Table 1). This represented 39/43 bony lesions, 1/5 liver metastases (Fig. 1) and 3/4 lung metastases. The false-negative bone metastases occurred in sites overlying the liver and may have been obscured by liver activity. An additional 11 foci of uptake were seen by antibody imaging. Of these, five were confirmed as metastatic disease using either plain films, MRI or bone scintigraphy (Fig. 2). These occurred in skeletal sites. Although blood pool persisted at 72 hr post-antibody administration, all tumors which were identified on the scan were evident by that time.

TABLE 4
Baseline BrE-3 Antigen Levels and Average HMW Complex Formation After Antibody Infusion

Dose level	BrE-3 antigen (μg/ml) [†]	% HMW*
10 mg	0.13	3.4%
	0	3.9%
	1.08	49%
	5.52	51.2%
	2.28	27.4%
50 mg	0.18	7.4%
	0	0.1%
	61.2	68.5%
	42.3	45.5%
	1.2	3.9%
100 mg	1.0	2.2%
	1.0	4.0%
	0	1.5%
	0.8	0.9%
	1.3	3.7%

*Mean percent radioactivity associated with high molecular weight complex (HMW) in serum samples after radiolabeled antibody administration.

[†]Antigen levels determined on serum samples obtained prior to antibody administration.

TABLE 5
Serum Pharmacokinetics (mean \pm s.e.)

Dose level	$T_{1/2\alpha}$ (hr)	$T_{1/2\beta}$ (hr)	AUC ($\mu\text{g/ml/hr}$)	% Beta	Clearance (ml/min/m ²)
10 mg	10.4 \pm 4.6	50.7 \pm 7.8	66.0 \pm 22.1	88.3 \pm 4.1	0.40 \pm 0.04
50 mg	8.7 \pm 4.4	46.2 \pm 12.3	249.7 \pm 107.5	79.1 \pm 4.0	0.72 \pm 0.23
100 mg	9.4 \pm 5.8	77.6 \pm 10.6	633.3 \pm 100.8	83.6 \pm 3.6	0.45 \pm 0.09
All doses	9.5 \pm 2.7	56 \pm 25.4	316.3 \pm 296.0	83.7 \pm 2.3	0.52 \pm 0.09

Serum BrE-3 Antigen Levels

At baseline, detectable serum levels of BrE-3 antigen were found in 12/15 patients with levels ranging from 0.1 to 61.2 $\mu\text{g/ml}$ (Table 4). In nine patients, serum obtained through 1 wk postadministration of the BrE-3 antibody was available for analysis of antigen levels. In two of the six patients who had detectable baseline levels, decreased but measurable levels of free antigen were detected after the administration of the antibody. In one of these two patients, detectable antigen levels reappeared at 6 days after BrE-3 antibody administration. In the other, in whom the baseline level was quite high (61.2 $\mu\text{g/ml}$), detectable levels were present throughout the initial week although they decreased quite markedly initially after infusion.

There was no significant correlation found between $T_{1/2\alpha}$, $T_{1/2\beta}$, clearance or %AUC described by the beta half-life and serum antigen levels. In the five patients with radioactive high molecular weight complexes in serum after antibody administration, the percent of radioactivity present as complexes could be predicted by the baseline serum antigen level and the mass of antibody administered.

HAMA

HAMA was measured after administration of antibody in 15 patients. Two of these patients showed very low serum HAMA (IgG) levels as early as a week after infusion. By 1 mo after administration, a total of five showed elevated HAMA levels and by 3–6 mo after administration, an additional two patients became positive. In addition to elevation of IgG, elevated IgE HAMA levels were found in two of the positive patients. Elevated levels of HAMA occurred at all antibody dose levels.

DISCUSSION

On a per lesion basis, ¹¹¹In-MX-DTPA BrE-3 showed a higher detection rate for known tumors than other antibodies directed against similar antigens in breast carcinoma (9) or antibodies directed against different breast associated antigens. We were able to visualize antibody localization by scan in at least one known lesion in 12/15 patients. In two patients with completely false-negative results, disease was confined to the liver. In a third patient with false-negative scans, lung and liver disease was present. The remaining false-negative lesions were either liver metastases which were seen as photopenic regions or bony lesions obscured by overlying liver activity. In one patient, a liver metastasis was demonstrated as an area of increased accumulation (Fig. 1). This was the only true-positive liver

metastasis. Detection rates were highest for bony lesions. Although we cannot be certain that this represents specific antibody localization, in at least one patient, the antibody study detected more skeletal lesions than the bone scan (Fig. 2). Localization in chest wall lesions was demonstrated uniformly well by antibody imaging (Fig. 3).

The estimated percent injected dose (%ID) localized in tumors as assessed by region of interest image analysis varied from 0.004% (in a 140-g tumor) to 0.28% ID/g. The higher estimates were obtained in relatively small tumors (e.g., 8 g). Although these estimates are in the range for accumulation reported for other radiolabeled antibodies, more accurate measurements of %ID/g tumor will be obtained in future therapy trials where tumor biopsies are planned. Based on these estimates and the assumption that tumor uptake of ⁹⁰Y-MX-DTPA-BrE-3 would be similar to that of ¹¹¹In-MX-DTPA-BrE-3, tumor radiation dose estimates for ⁹⁰Y-MX-DTPA-BrE-3 were made for measurable tumors. These estimates ranged from 5.2 rads to 590 rads/mCi, averaging 109 \pm 149 rads/mCi.

Based on these results, tumoricidal doses theoretically could be administered to some patients with 20 mCi of

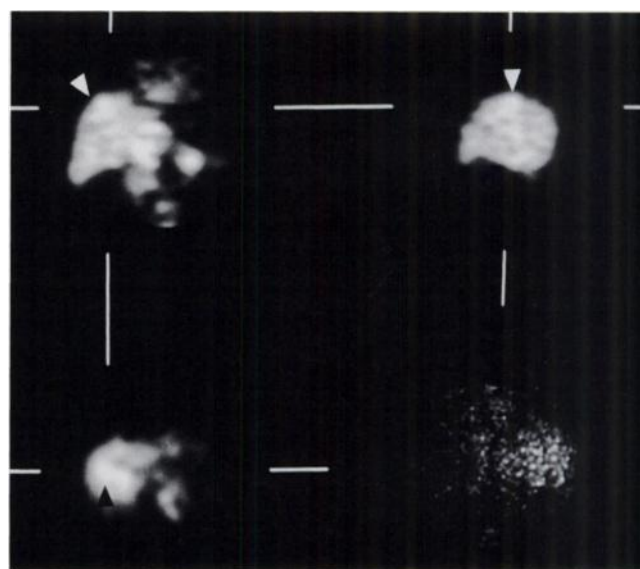


FIGURE 1. Coronal (upper left), transaxial (lower left) and sagittal (upper right) slices from the SPECT study 72 hr after radiolabeled antibody administration in a 62-yr-old woman with a history of mastectomy for Stage II carcinoma of the breast. Increased uptake in the liver (arrowheads) corresponds in location to the known metastasis seen on CT. On the coronal slice, increased uptake in bilateral adrenal gland metastases may also be appreciated. These also were identified on previous CT.

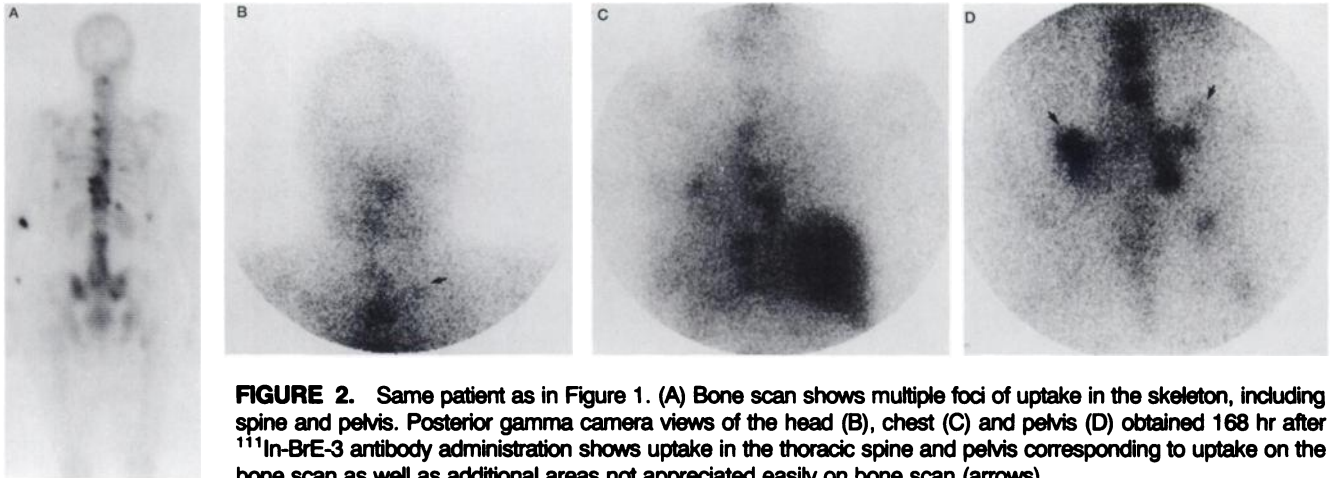


FIGURE 2. Same patient as in Figure 1. (A) Bone scan shows multiple foci of uptake in the skeleton, including spine and pelvis. Posterior gamma camera views of the head (B), chest (C) and pelvis (D) obtained 168 hr after ^{111}In -BrE-3 antibody administration shows uptake in the thoracic spine and pelvis corresponding to uptake on the bone scan as well as additional areas not appreciated easily on bone scan (arrows).

^{90}Y -MX-DTPA-BrE-3. Average radiation dose estimates from these 20 mCi to liver were 184 rads, to lung 168 rads, to spleen 307 rads and to kidneys 129 rads. Based on the ^{111}In -MX-DTPA-BrE-3 images and blood pharmacokinetics and assuming similar ^{90}Y -MX-DTPA-BrE-3 localization, the calculated radiation dose delivered to red marrow from 20 mCi of ^{90}Y -MX-DTPA-BrE-3 was 41 rads. This estimate accounts only for radiation dose due to radioisotope circulating in the blood. However, estimates of marrow dose from ^{90}Y -MX-DTPA-BrE-3 made using ^{111}In MX-DTPA BrE-3 biodistribution are expected to be inaccurate since there is bone matrix localization of free ^{90}Y in addition to circulating radioisotope (26). Bone and marrow biopsy measurement with quantitative autoradiography may be necessary to enable more accurate dosimetry calculations.

One of the expected advantages of BrE-3 antibody was the relatively lower levels of circulating antigen recognized by this antibody compared to the levels of the epitope recognized by Mc5. Although other authors have shown that circulating antigen, e.g., CEA or TAG-72, in small to moderate quantities does not interfere with antibody localization in tumor (27), large amounts of circulating antigen may interfere. This was demonstrated in studies with Mc5 where large amounts of circulating antigen bound most of the administered antibody. Five of our 15 patients showed significant (>20%) high molecular weight (~450 kD) com-

plexes in serum which probably represents antigen antibody complex. In four of these five patients, the measured circulating antigen level prior to antibody administration predicted this complex formation (Table 4). In all but one patient, high molecular weight (HMW) complex peaked by the end of infusion.

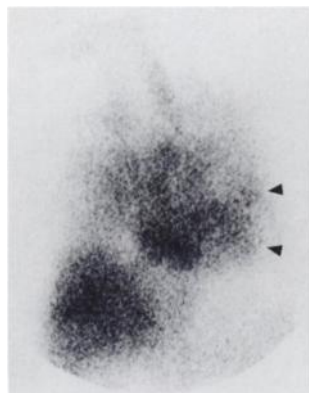
The presence of these levels of circulating antigen did not seem to interfere with the ability to localize tumor by scan. Although higher levels of high molecular weight complex were associated with a shorter serum biological half-life for antibody, the correlation was not significant ($r = -0.41$). Similarly, antibody half-life in tumor tended to be somewhat shorter as the percent of HMW complex increased, but again the correlation was not significant.

Since the pharmacokinetic parameters did not differ significantly among dose levels, the dose level for future studies was selected based on the theoretical advantage of administering amounts of antibody which will exceed the binding capacity of circulating antigen. Only 2 of the 15 patients studied had BrE-3 antigen levels >10 $\mu\text{g}/\text{ml}$. Serum antigen concentrations of 10 $\mu\text{g}/\text{ml}$ would be expected to saturate approximately 20% of a 50-mg dose of antibody, thereby leaving the remainder available for tumor localization.

Furthermore, the safety of administering these dose levels of BrE-3 antibody was shown. Although the incidence of allergic reactions was slightly higher in this small group than those described with some other murine Mab, one of the reactions was related to a rapid infusion rate and the other two reactions were quite mild.

Radioimmunodetection in the staging of primary breast carcinoma, particularly in evaluation of regional lymph nodes, could offer information important for predicting prognosis and in treatment planning. Prior studies attempting to use radiolabeled antibodies to accurately assess lymph node involvement in breast cancer have not been successful. Intravenously administered radiolabeled antibodies directed against TAG-72 have not shown high accuracy in identifying lymph node involvement (28). Interstitial administration of CEA-specific whole antibodies in

FIGURE 3. A 73-yr-old woman with a history of an infiltrating ductal carcinoma of the left breast with a recurrence in the left chest wall. Anterior view of the chest 96 hr after intravenous administration of approximately 5 mCi of ^{111}In -MX-DTPA-BrE-3 antibody shows accumulation in the left chest wall mass (arrowheads).



patients with primary breast carcinoma have shown non-specific uptake (2-3). More recently, subcutaneous (web space) administration of F(ab')₂ fragments of HMFG₁ and HMFG₂ antibodies have yielded more accurate results (6). Intravenous administration of these same radiolabeled F(ab')₂ fragments, however, has resulted in localization in less than half of the primary lesions, in only two-thirds of bony lesions and been less successful in detecting lymph node metastases (9). Similar results have been achieved with other ¹¹¹In-labeled whole antibodies directed against an epitope of the breast mucin (7). BrE-3 antibody may offer advantages over these antibodies for initial staging since higher detection rates were achieved with intravenously administered BrE-3 in metastatic and recurrent disease in this study.

This may be due in part to the lack of interference from overwhelming levels of circulating antigen and to the abundance of the epitope recognized by this antibody in tumor tissue. The level of glycosylation of the epitope may play an important role in targeting breast tumors. Full or complete glycosylation of the breast epithelial mucin occurs in its more mature form found in HMFG, but not in breast tumor cells (29). It can be hypothesized that an increased availability of a less glycosylated epitope, such as the one detected by BrE-3 (30) as compared to Mc-5, for example, could contribute to successful breast tumor targeting. Mc-5, whose epitope was shown to have a high level of carbohydrate contribution to its structure (30), was not successful for breast tumor imaging (17). In contrast, the epitope of BrE-3 does not appear to have any carbohydrate contribution to its structure (30), thus making the BrE-3 epitope more prevalent in breast cancer cells and more tumor specific.

Also, the use of the isothiocyanatobenzyl-methyl DTPA ¹¹¹In chelate, which has been shown to have higher stability in vivo than the DTPA anhydride (31), may contribute to the improved tumor localization with BrE-3. In our patients, average liver accumulation of ¹¹¹In was below that reported in other studies using a DTPA anhydride chelate (20%) (9,19).

The clinical role of radioimmunodetection in the evaluation of metastatic disease or recurrence is less clear. The sensitive detection of metastases after recurrence may not change therapy at this time. Statistical data on disease outcome in patients with breast cancer suggest that with the currently available therapeutic modalities, detection of metastases will have little clinical impact since patients who have recurrent or metastatic breast cancer after first treatment will die of their disease. However, if new therapies such as radioimmunotherapy combined with other high dose multimodality approaches can be developed for initial recurrent and/or minimal disease, then ¹¹¹In-labeled antibodies might play a role in recurrent disease staging. Furthermore, the use of the ¹¹¹In-labeled antibody for radioimmunolocalization may prove to be helpful in predicting tumor dosimetry and the therapeutic index in radio-

immunotherapy with the same chelate conjugate and antibody.

It is in the realm of therapy that radiolabeled antibodies could have significant impact. Some early success of radioimmunotherapy in aggressive recurrent/metastatic disease has been achieved (21,32). Because of the abundant expression of this antigen on most breast cancers and the good tumor localization in vivo, BrE-3 labeled with an appropriate therapeutic isotope like ⁹⁰Y, may be a useful therapeutic in patients who have failed their first line therapy for metastatic disease. A Phase I radioimmunotherapy trial of ⁹⁰Y-MX-DTPA-BrE-3 in patients with advanced breast cancer is underway. The role of radioimmunotherapy in less refractory, less advanced disease and as part of a multimodality approach must be defined further as we gain experience with this type of cancer therapy.

ACKNOWLEDGMENTS

This work was funded by the National Cancer Institute primarily through 3PO1-CA42767 awarded to the Cancer Research Fund of Contra Costa. Additional support was provided through R01-CA39932. The authors would like to acknowledge the clinical support of Dr. Christina Walsh and Andrea Downey, RN. Dr. Joseph Sanger provided assistance and advice on the nuclear medicine acquisitions. Dr. Gregory Butchko lent administrative support for antibody production and development of quality control procedures. Edward Blank provided untiring and invaluable help and advice in the laboratory. Gary Mirick provided invaluable assistance with the radiation dosimetry calculations. The authors also are indebted to Raghavan Sampathkumaran, Evelyn Millan, Jeffrey Davis, Cathy Suey, Denise Neverla, Jeffrey Schwimmer, Robert Bae for technical assistance and to Linda Melnikoff and Julie Skaug for their efforts in data management. We also thank Drs. Ronald Blum, James Speyer, James Wernz and Ruth Oratz for clinical support.

REFERENCES

1. Goldenberg DM, DeLand FH, Kim EE, et al. Use of radiolabeled antibodies to carcinoembryonic antigen for the detection and localization of diverse cancers by external photoscanning. *N Engl J Med* 1978;298:1384-1388.
2. Deland FH, Kim EE, Corgan RL, et al. Axillary lymphoscintigraphy by radioimmunodetection of carcinoembryonic antigen in breast cancer. *J Nucl Med* 1979;20:1243-1250.
3. Deland FH, Kim EE, Goldenberg DM. Lymphoscintigraphy with radionuclide-labeled antibodies to carcinoembryonic antigen. *Cancer Res* 1980;40:2997-3000.
4. Hayes DF, Zalutsky MR, Kaplan W, et al. Pharmacokinetics of radiolabeled monoclonal antibody B6.2 in patients with metastatic breast cancer. *Cancer Res* 1986;46:3157-3163.
5. Riva P, Moscatelli G, Paganelli G, et al. Antibody-guided diagnosis: an Italian experience on CEA-expressing tumors. *Int J Cancer* 1988;2(suppl):114-120.
6. Athanassiou A, Pectasides D, Pateniotes K, et al. Immunoscintigraphy with ¹³¹I-labeled HMFG2 and HMFG1 (Fab')₂ in the pre-operative detection of clinical and subclinical lymph node metastases in breast cancer patients. *Int J Cancer* 1988;3(suppl):89-95.
7. Rainsbury RM. The localization of human breast carcinomas by radiolabelled monoclonal antibodies. *Br J Surg* 1984;71:805-812.
8. Epenetos AA, Mather S, Granowska M, et al. Targeting of iodine-123-labelled tumour-associated monoclonal antibodies to ovarian, breast, and gastrointestinal tumours. *Lancet* 1982;2:999-1005.
9. Kalafonos HP, Sackier JM, Hatzistylianou M, et al. Kinetics, quantitative analysis and radioimmunolocalisation using indium-111-HMFG1 monoclonal antibody in patients with breast cancer. *Br J Cancer* 1989;59:939-942.
10. Mandeville R, Pateisky N, Philipp K, et al. Immunolymphoscintigraphy of

axillary lymph node metastases in breast cancer patients using monoclonal antibodies: first clinical findings. *Anticancer Res* 1986;6:1257-1263.

11. Ceriani RL, Peterson JA, Lee JY, Moncada R, Blank EW. Characterization of cell surface antigens of human mammary epithelial cells with monoclonal antibodies prepared against human milk fat globule. *Somat Cell Genet* 1983;9:415-427.
12. Peterson JS, Zava DT, Duwe AK, et al. Biochemical and histological characterization of antigens preferentially expressed on the surface and cytoplasm of breast carcinoma cells identified by monoclonal antibodies against the human milk fat globule. *Hybridoma* 1990;9:221-235.
13. Ceriani RL, Peterson JA, Blank EW, Chan CM, Cailleau R. Development and characterization of breast carcinoma cell lines as in vitro and in vivo models for breast cancer diagnosis and therapy. *In Vitro* 1993;28A:397-402.
14. Ceriani RL, Sasaki M, Orthendahl D, Kaugman L. Localization of human breast tumors grafted in nude mice with a monoclonal antibody directed against a defined cell surface antigen of human mammary epithelial cells. *Breast Cancer Res Treat* 1988;12:177-189.
15. Ceriani RL, Blank EW, Peterson JA. Experimental immunotherapy of human breast carcinomas implanted in nude mice with a mixture of monoclonal antibodies against human milk fat globule components. *Cancer Res* 1987;47:532-540.
16. Ceriani RL, Blank EW. Experimental therapy of human breast tumors with ¹³¹I-labeled monoclonal antibodies prepared against the human milk fat globule. *Cancer Res* 1988;48:4664-4672.
17. Bunn PA Jr, Dienhart DG, Gonzalez R, et al. Imaging, pharmacokinetics and antitumor effects of radiolabelled anti-breast cancer antibodies in mouse and man. In: Ceriani RL, ed. *Breast epithelial antigens*. New York: Plenum Press; 1991:227-232.
18. Blank EW, Pant KD, Chan CM, Peterson JA, Ceriani RL. A novel anti-breast epithelial mucin MoAb (BrE-3). Characterization and experimental biodistribution and immunotherapy. *Cancer J* 1992;5:38-44.
19. Macey DJ, DeNardo SJ, DeNardo GL, Goodnight JK, Unger MW. Uptake of indium-111-labeled monoclonal antibody ZME-018 as a function of tumor size in a patient with melanoma. *Am J Phys Imag* 1988;3:1-6.
20. Macey DJ, DeNardo GL, DeNardo SJ. A Treatment Planning Program for Radioimmunotherapy. In: Vaeth JM, Meyer JL, eds. *The present and future role of monoclonal antibodies in the management of cancer*, volume 24. Basel: Karger; 1990:123-131.
21. DeNardo SJ, Warhoe KA, O'Grady LF, et al. Radioimmunotherapy for breast cancer: treatment of a patient with I-131 L-6 chimeric monoclonal antibody. *Int J Biol Markers* 1991;6:221-230.
22. Watson EE, Stabin M, Bolch WE. MIRDose, version 2. Oak Ridge, TN: Oak Ridge Associated Universities; 1984.
23. Brownell GL, Ellett WH, Reddy AR. Absorbed fractions for photon dosimetry. *MIRD pamphlet no. 3. J Nucl Med* 1968;9(suppl 1):27-39.
24. Snyder WS, Ford MR, Warner GG, Watson SB. MIRD pamphlet no. 11: "S", absorbed dose per unit cumulated activity for selected radionuclides and organs. Oak Ridge, TN: Oak Ridge National Lab; 1975.
25. Dienhart DG, Bloedow DC, Hartmann C, et al. A phase I trial of KC-4 monoclonal antibody serotherapy of advanced non-small cell lung and breast cancers: clinical, pharmacokinetic, and immunologic results. *Cancer Res* 1993; in press.
26. Roselli M, Schlom J, Gansow OA, et al. Comparative biodistributions of yttrium- and indium-labeled monoclonal antibody B72.3 in athymic mice bearing human colon carcinoma xenografts. *J Nucl Med* 1989;30:672-682.
27. Carrasquillo JA, Sugarbaker P, Colcher D, et al. Radioimmunoscintigraphy of colon cancer with iodine-131-labeled B72.3 monoclonal antibody. *J Nucl Med* 1988;29:1022-1030.
28. Lamki LM, Buzdar AU, Singletary SE, et al. Indium-111-labeled B72.3 monoclonal antibody in the detection and staging of breast cancer: a phase I study. *J Nucl Med* 1991;32:1326-1332.
29. Hull SR, Bright A, Carraway KL, Abe M, Hayes DF, Kufe DW. Oligosaccharide differences in the DF3 sialomucin antigen from normal human milk and the BT-20 human breast carcinoma cell line. *Cancer Commun* 1989;1:261-267.
30. Ceriani RL, Peterson JS, Lamport D, Amiya R. Epitope expression on the breast epithelial mucin. *Breast Cancer Res Treat* 1993;24:103-113.
31. Brechbiel MW, Gansow OA, Atcher RW, et al. Synthesis of 1-(p-isothiocyanatobenzyl) derivatives of DTPA and EDTA. Antibody labeling and tumor-imaging studies. *Inorg Chem* 1986;25:2772.
32. DeNardo SJ, Warhoe KA, O'Grady LF, et al. Radioimmunotherapy with I-131 chimeric L-6 in advanced breast cancer. In: Ceriani RL, ed. *Breast epithelial antigens*. New York: Plenum Press; 1991:215-225.